Optical control of an ion channel gate

Damien Lemoine[a,b], Chloé Habermacher[a,b], Adeline Martz[a,b], Pierre-François Méry[c,d,e], Nathalie Bouquier[c,d,e], Fanny Diverchy[a,b], Antoine Taly[f,g], François Rassendren[c,d,e,h], Alexandre Specht[a,b], and Thomas Grutter[a,b,1]

[a]Centre National de la Recherche Scientifique, Unité Mixte de Recherche 7199, Laboratoire de Conception et Application de Molécules Bioactives, Équipe de Chimie et Neurobiologie Moléculaire, F-67400 Illkirch, France; [b]Université de Strasbourg, Faculté de Pharmacie, F-67400 Illkirch, France; [c]Centre National de la Recherche Scientifique, Unité Mixte de Recherche 5203, Institut de Génomique Fonctionnelle, F-34000 Montpellier, France; [d]Institut National de la Santé et de la Recherche Médicale U661, F-34000 Montpellier, France; [e]Universités de Montpellier 1 and 2, F-34000 Montpellier, France; [f]Centre National de la Recherche Scientifique, Laboratoire de Biochimie Théorique, F-75005 Paris, France; [g]Université Paris Diderot, F-75005 Paris, France; [h]Laboratory of Excellence Ion Channel Science and Therapeutics (LabEx ICST), F-34000 Montpellier, France

Edited by Richard W. Aldrich, University of Texas at Austin, Austin, TX, and approved November 8, 2013 (received for review October 3, 2013)

The powerful optogenetic pharmacology method allows the optical control of neuronal activity by photoswitchable ligands tethered to channels and receptors. However, this approach is technically demanding, as it requires the design of pharmacologically active ligands. The development of versatile technologies therefore represents a challenging issue. Here, we present optogating, a method in which the gating machinery of an ATP-activated P2X channel was reprogrammed to respond to light. We found that channels covalently modified by azobenzene-containing reagents at the transmembrane segments could be reversibly turned on and off by light, without the need of ATP, thus revealing an agonist-independent, light-induced gating mechanism. We demonstrate photocontrol of neuronal activity by a light-gated, ATP-insensitive P2X receptor, providing an original tool devoid of endogenous sensitivity to delineate P2X signaling in normal and pathological states. These findings open new avenues to specifically activate other ion channels independently of their natural stimulus.

azobenzene photoswitch | purinergic receptors

Optogenetic approaches in neuroscience rely on the heterologous expression of engineered light-gated ion channels or pumps to trigger or inhibit electrical activity of selected neurons (1, 2). This powerful and revolutionizing technique provides an exquisite remote control of neuronal circuits that drive behavior in animals. Of special interest is the optogenetic pharmacology (also known as optochemical genetic) (3, 4), which allows the control of an ion channel or receptor function by a photoswitchable ligand that is irreversibly tethered to the genetically modified protein through cysteine substitution (3, 4). Ligands are pharmacologically active substances targeting either competitive (5–7), or noncompetitive binding sites (8–10), and light sensitivity is mostly conferred by substituting a photoisomerizable azobenzene derivative, which interconverts reversibly between a long *trans*-isomer and a short *cis*-isomer (11). However, this approach is technically demanding, as it requires the design of site-specific ligands for each target. The development of versatile methods with generic photoswitchable molecules would thus improve the optochemical strategy.

Here, we present optogating, a unique method for the optical control of ATP-activated P2X channel gating. P2X receptors are a family of trimeric, cation-selective channels (12, 13) comprising seven mammalian subtypes that mediate a variety of physiological responses, including fast synaptic transmission, contraction of smooth muscle, modulation of neurotransmitter release, and pain sensation (12, 14, 15). P2X receptors are considered as emerging therapeutic targets because of their link to cancer (16), inflammatory (17), and neuronal diseases, including neuropathic pain (18). Inspired by previous works showing that chemical modification of the transmembrane (TM) pore region of the P2X2 receptor affects channel gating through labeling of single cysteine mutants by positively charged methanethiosulphonate reagents (19–21), we sought to optically control the gating machinery of the receptor by covalently introducing into the same region positively charged, azobenzene-containing photoswitches. We found that engineered channels could be reversibly turned on and off by light, without the need of ATP, revealing a unique ATP-independent, light-induced gating mechanism. We applied our system in cultured hippocampal neurons, and showed that a light-gated P2X2 receptor that was made genetically insensitive to endogenous ATP rapidly and reversibly photomodulated synaptic activity and action potential firing. These findings establish original tools to delineate P2X receptor signaling in vivo, and provide new opportunities to specifically activate by light other ion channels in which the endogenous sensitivity of the natural signal can be genetically removed.

Results

Design of the Optogating Approach. To design the optogating strategy, we synthesized the sulfhydryl reactive, maleimide ethylene azobenzene trimethyl ammonium derivative (MEA-TMA) (Fig. 1*A* and Fig. S1). This molecule is similar to maleimide azobenzene quaternary ammonium (MAQ), a compound initially developed to optochemically control K^+ channels activity (8). MEA-TMA rapidly photoisomerized in solution from the dark-adapted *trans*-isomer to the *cis*-isomer by using a 365-nm light, and photoswitched back to the *trans*-isomer either rapidly by a 525-nm light or slowly by thermal relaxation (k_BT) in the dark (Fig. S2). We selected 19 residues, including those previously identified (19, 20), from the outer region of transmembrane segments TM1 and TM2 (Table S1), and substituted each of them with a cysteine into the P2X2-3T background, a functional receptor in which three native cysteine residues (one in TM2 and one in each of the two termini) were mutated to threonine (20). Following transient expression in HEK cells, all single cysteine mutants responded robustly to ATP

Significance

Engineered light-sensitive ion channels offer the opportunity to govern electrical activity of neurons. To date, developed strategies have relied on specific actions on either ligand-binding or permeation pathways. Here we developed a unique and versatile method, in which the gating machinery of an ATP-activated channel (purinergic P2X receptor) was reprogrammed to respond to light. We found that channels covalently modified by azobenzene-containing reagents at the transmembrane segments could be reversibly turned on and off by light, without the need of the natural ligand (here ATP). We demonstrate photocontrol of neuronal activity by a light-gated P2X receptor, in which the natural sensitivity to ATP was genetically removed. These light-gated P2X receptors represent valuable tools for investigating their physiological functions.

Author contributions: D.L., C.H., P.-F.M., A.T., F.R., A.S., and T.G. designed research; D.L., C.H., A.M., P.-F.M., N.B., F.D., A.T., F.R., and A.S. performed research; D.L., C.H., P.-F.M., A.S., and T.G. analyzed data; and F.R., A.S., and T.G. wrote the paper.

The authors declare no conflict of interest.

This article is a PNAS Direct Submission.

[1]To whom correspondence should be addressed. E-mail: grutter@unistra.fr.

This article contains supporting information online at www.pnas.org/lookup/suppl/doi:10.1073/pnas.1318715110/-/DCSupplemental.

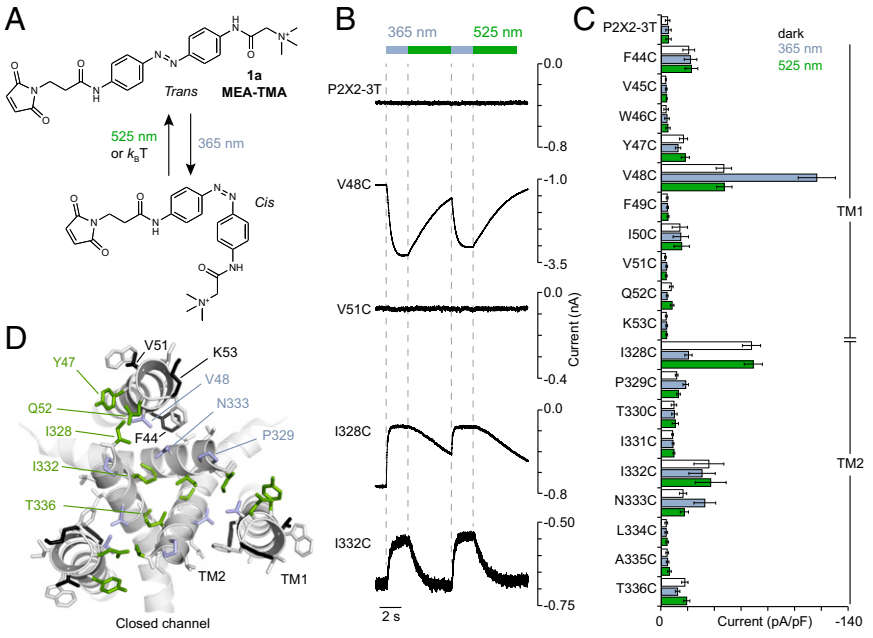

Fig. 1. Tethered MEA-TMA turns on and off the P2X2 channel by light. (*A*) Chemical structure and *cis-trans* isomerization of MEA-TMA. (*B*) Whole-cell currents evoked by light at the indicated wavelengths in HEK cells expressing the indicated constructs that were prior-treated to MEA-TMA in the dark. For V48C, labeling was performed in the presence of ATP. (*C*) Screening for all constructs showing current density recorded in the dark, followed by 365- (violet bars) and 525-nm (green bars) light illuminations (n = 4–7 cells; mean ± SEM). (*D*) Mapping of switchable positions viewed from the extracellular side along the threefold axis of symmetry of a closed-channel state P2X2 homology model reveals *trans*- and *cis*-openers, colored as green and violet sticks, respectively. Gray- and black-colored sticks indicate, respectively, selected and labeled residues with no effect upon light irradiation. TM1 and TM2 α-helices from the same subunit are also indicated.

as determined by patch-clamp electrophysiology, and exhibited half-maximal effective concentrations (EC_{50}) of ATP that were similar to those previously determined (20) (Table S1).

After MEA-TMA labeling in the dark followed by extensive washing (see *Materials and Methods* for labeling procedure), we noticed that cells expressing some mutants displayed, immediately after break-in, a leak of the holding current that could be either decreased (for Y47C, Q52C, I328C, I332C, and T336C mutants) or increased (V48C, P329C and N333C) upon 365-nm light illumination (Fig. 1 *B* and *C*, and Fig. S3). Irradiation at 525 nm reversed these UV-modified holding currents, and repeated toggling between 365- and 525-nm lights robustly switched these currents back and forth, thus revealing potent *cis*- or *trans*-openers. Amplitudes of the light-gated currents depended on the mutant position in the channel, and ranged from small to robust photocurrents (Fig. 1 *B* and *C* and Table S1). In contrast, we did not observe any leak or photoactivation in untreated cells expressing these mutants. Furthermore, treatment of the remaining 11 mutants, including the P2X2-3T, with MEA-TMA did not convey self-photosensitivity to the receptors (Fig. 1 *B* and *C*).

When mapped on the closed-channel state homology model, built from the recent X-ray structure of the zebrafish P2X4 receptor (22), *trans*-openers were placed between TM2 α-helices from two adjacent subunits, whereas *cis*-openers were mostly located between TM1 and TM2 α-helices from the same subunit (Fig. 1*D*). Thus, the optogating method identifies several positions in the P2X2 pore that optically fine-tune the gating machinery of the channel at either short or long wavelength.

For F44C and V48C mutants, substantial leak currents that did not decrease upon light illumination were recorded in the dark (Fig. 1*C* and Table S1). The reason for this result is unclear, but may be related to the fact that the two residues are separated by one-helix turn in TM1 (Fig. 1*D*). As these leak currents were minimal in the absence of MEA-TMA labeling (−8.9 ± 2.1 pA/pF for F44C, and −7.3 ± 3.5 pA/pF for V48C, n = 3–4), and because side-chains of F44 and V48 face TM2 α-helices that form the ion channel in the open state, one may speculate that their chemical modifications by the dark-adapted *trans*-isomer would destabilize interactions between these helices in the closed state, thus producing some channel openings. Additional experiments are needed to clarify this issue.

Tethered Photoswitchable Reagents Rapidly Gate P2X2 Channel. An important requirement to achieve precise optical gating of ion channels is that activation and inactivation kinetics induced by light are in the same range as those observed in physiological conditions. We thus investigated the kinetics of photoactivation and inactivation by measuring time constants (τ) of currents recorded at different wavelengths. Depending on the attachment points in the channel, we found that these constants ranged from 1.38 ± 0.25 to 12.3 ± 3.2 s at 525-nm light, and from 0.090 ± 0.003 to 0.335 ± 0.037 s at 365-nm light (Table S1). However, we observed that increasing 525-nm light intensity from 0.36 to 4.5 mW/mm^2 to cells expressing the I328C mutant, which was one of the slowest mutants to activate at this wavelength, decreased by more than 10-times τ values (from 4.22 ± 0.33 to 0.36 ± 0.02 s, n = 4 cells), but without affecting photocurrent amplitude (Fig. 2 *A* and *B*). These observations show that tethered photoswitches can rapidly gate P2X2 channels (time to reach maximal current is ∼1 s at 4.5 mW/mm^2), although these apparent rates were slower than those previously determined at saturating concentration of ATP (∼80 ms) (23).

A second requirement for an in vivo or ex vivo use is that optical gating of channels remains stable, with little thermo relaxation of the *cis*- to the *trans*-isomer, in particular in the closed-channel state. We thus analyzed whether photo-induced closed state was stable in the absence of illumination by measuring for I328C mutant currents recorded in the dark. Channel closure achieved by the *cis*-isomer was stable in the dark for at least 60 s, until 525-nm illumination again promoted channel opening (Fig. 2*C*). These results indicate that the kinetics of thermal relaxation from the *cis*- to the *trans*-isomer measured in solution are considerably slowed down once bound to the protein. In addition, when receptors were turned on by 525-nm illumination, channels remained open in the dark for at least 20 s (Fig. 2*C*). These persistent effects demonstrate bistability of the optogating method, a key feature that was already observed for other receptors (6, 24); it allows tethered azobenzenes to remain in the dark either in their *cis* or *trans* isomer following brief illuminations. These data establish a stable photocontrol of channels.

Tethered Photoswitchable Reagents Modulate ATP Responses. To explore the mechanisms underlying light activation, we first investigated the effect of light on responses elicited by ATP (measured at the EC_{50}). All mutants that were endowed with light sensitivity in ATP-free solutions displayed consistent *trans*- or *cis*-blockage of the ATP-evoked responses, except Q52C and N333C mutants, for which switching light had no detectable effect on

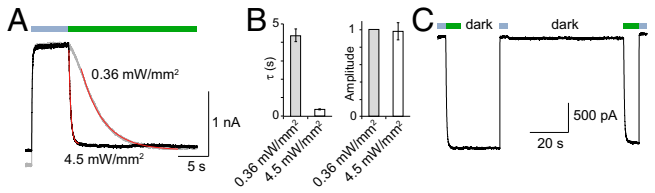

Fig. 2. Kinetics and bistability of azobenzene isomerization attached at the I328C mutant. (*A*) Increasing 525-nm light intensity (green bar) to a cell expressing the I328C mutant tethered to MEA-TMA increases activation rates of whole-cell current. Data were fitted by single exponential decay functions (in red). (*B*) Bar plot summarizing data presented in *A* shows substantial change of time constant (τ) but not of light-induced current amplitude (normalized to 0.36 mW/mm^2) ($n = 4$ cells; error bars are SEM). (*C*) Bistability of light-induced currents revealed in the dark following brief photoactivation at 525 nm (green bars, light intensity was set to 4.5 mW/mm^2) and brief inactivation at 365 nm (violet bars) in a cell expressing the I328C mutant tethered to MEA-TMA. Note that the basal current is stable in the dark until a new photoactivation of similar amplitude occurs.

ATP currents (Fig. 3*A*, Fig. S3, and Table S1). From a homology model of an open-channel state built from the ATP-bound crystal structure (22), all *trans*-blockers of ATP-evoked currents were positioned at an external ring from the central threefold axis of symmetry, whereas most of the *cis*-blockers were positioned at a more internal ring (Fig. 3*B*). These results are consistent with the hypothesis that the positive charge of MEA-TMA repels cation flux through the conducting pathway, through a mechanism that closely depends upon the relative distance to the open pore induced by ATP. In particular, docking of MEA-TMA on the active-state's model of the I328C mutant showed that the ability of the charge to occupy the constriction of the pore depended on the isomerization of the azobenzene (Fig. S4).

Next, we compared the mapping of photoswitchable positions recorded in the presence of ATP with that measured in its absence (compare Fig. 1*D* with Fig. 3*B*). A clearly different pattern of positions was revealed. First, *trans*-isomers tethered to Y47C or the I328C mutant opened the channel in the absence of ATP, but blocked ATP currents in its presence, indicating a state-dependent action of MEA-TMA (Figs. 1*B* and 3*A*, and Fig. S3). A detailed ATP dose–response analysis for the I328C mutant confirmed that the *trans*-isomer reduced by up to 68 ± 6% the maximal ATP currents with a slight increase of ATP potency ($EC_{50–525\ nm} = 1.5 \pm 0.4$ μM; $EC_{50–365\ nm} = 2.8 \pm 0.7$ μM, $n = 5$ cells) (Fig. 3*C*). Second, photoswitches tethered to the V51C and K53C mutants were not openers in ATP-free solution, but modified ATP responses, demonstrating that these labeled residues are unable to induce substantial photoactivation on their own (Figs. 1*B* and 3*A*, and Fig. S3). Because V51 and K53 residues are located more extracellularly in the channel than I328, these data suggest that the direct photoactivation acts further downstream from this position, most likely at the level of the TM α-helices where critical residues have been identified as important for gating (19, 20, 25, 26). Taken together, these data support the existence of two light-gated mechanisms occurring independently: one that is produced in the presence of ATP and acts through a pore-blocking mechanism, and a second one that occurs without the need of ATP and acts directly on the gate of the channel.

Exploring the Light-Gated, ATP-Independent Mechanism. To further gain insight into the ATP-independent, light-gated mechanism, we assessed the ability of a series of synthesized azobenzene derivatives, including MAQ (8), that differ in their structure and formal charge to directly gate the channel (Fig. 4*A* and Fig. S1). We focused on the I328C mutant because it displayed the largest and more stable light-gated currents. Neither the length of the spacer arm nor the size of the positively charged group changed the photoactivation yield of the *trans*-opener compared with a saturating concentration of ATP (Fig. 4 *B* and *C*). In contrast, reversing the sign of the formal charge by substituting TMA with a sulfonate group (SO_3^-) dramatically affected photocurrent yield, but subsequent application of MEA-TMA essentially restored currents, suggesting that the level of MEA-SO_3 labeling was low (Fig. 4 *B* and *C*). This result is not surprising because negatively charged MEA-SO_3 has to cross a highly acidic extracellular vestibule to access the pore before labeling (22, 27). Increasing time incubation (up to 20 min) or concentration (1 mM) of MEA-SO_3 did not improve labeling yields. We obtained similar results with the noncharged compound MEA-OMe (Fig. 4), further emphasizing the critical role of the positive charge in efficient labeling.

Regardless of the labeling yields and, consequently, of current amplitudes, the qualitative similarity of photocurrents recorded with tethered compounds carrying either opposite or no charge suggests that isomerization of the azobenzene core is critical to the light-induced mechanism (Fig. 4*B*). We conclude from these experiments that the presence of the positive charge of photoswitch compounds enables efficient labeling of engineered receptors, and that toggling of tethered photoswitches promotes channel gating.

A Light-Gated, ATP-Insensitive Channel Conducts Cations. Our data show that engineered P2X2 receptors can be activated by light without the need of ATP. Based on this observation, we designed another construct that did not sense ATP, providing the opportunity

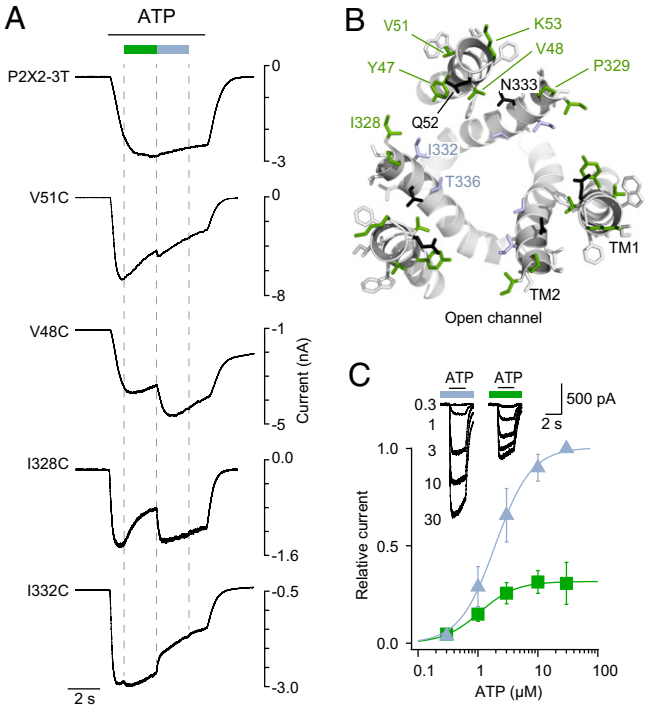

Fig. 3. Tethered MEA-TMA photomodulates ATP response of P2X2 channels. (*A*) Whole-cell currents evoked by ATP (EC_{50}) modulated by light in the same cells as those shown in Fig 1*B*. For I328C and I332C, cells were prior-irradiated with a short 4-s lasting pulse of 365-nm light to induce channel closure. (*B*) Same view as in Fig. 1*D*, in which *trans*- and *cis*-blockers colored, respectively, as green and violet sticks, are mapped on a P2X2 model in an ATP-bound, open-channel state. Gray- and black-colored sticks indicate, respectively, selected and labeled residues with no effect upon light irradiation on ATP response. (*C*) ATP dose–response curves recorded at 365-nm (violet) and at 525-nm light (green) from cells expressing the I328C mutant tethered with MEA-TMA ($n = 5$ cells; mean ± SEM). Currents were normalized to 30 μM ATP at 365 nm. (*Inset*) Typical superimposed ATP traces at the indicated illumination wavelengths.

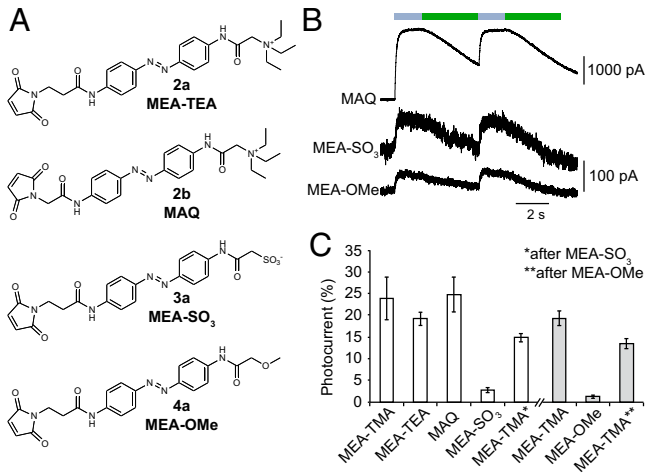

Fig. 4. Critical role of the photoswitch-positive charge for labeling P2X2 channels. (*A*) Chemical structures of MEA-TMA analogs. (*B*) Whole-cell currents evoked by light in cells expressing the I328C mutant tethered with MAQ, MEA-SO_3, or MEA-OMe, as indicated. (*C*) Bar plot showing photocurrent amplitudes elicited by 525-nm light normalized to currents evoked by a saturating concentration of ATP (recorded at 365-nm light) in cells expressing the I328C mutant tethered to the indicated MEA-TMA analogs. Labeling was performed with either 200 μM (white bars) or 80 μM (gray bars) of the analogs (n = 3–7 cells; mean ± SEM).

to express in neurons a light-gated P2X receptor devoid of endogenous activation. We introduced into the I328C background the K69A mutation, which is known to abolish ATP binding (28, 29), and showed that, as expected, no ATP current was measured although robust light-gated currents were still recorded following MEA-TMA treatment (Fig. 5*A*). We then asked whether the channel still conducts cations, because recent work has shown that introduction of positive charge into the pore, through mutation of residue T339 into lysine, converts the channel from being cation-selective to anion-preferring (30). We found that both MEA-TMA–tethered mutants I328C and K69A/I328C were still permeable to sodium and calcium ions (although calcium permeability was less than that measured for the WT P2X2 receptor) (31), but not to chloride ions (30, 32) (Fig. 5*B*, Fig. S5, and Tables S2 and S3), indicating that tethered MEA-TMA molecules do not alter cation selectivity of the channel.

P2X2 receptors are well known for undergoing "pore dilation" after prolonged ATP application, a process defined by increased permeability to large organic cations, such as *N*-methyl-D-glucamine (NMDG) (12, 33, 34). To determine whether light-gated receptors were also able to undergo such pore dilation following light illumination, we measured NMDG permeability 3, 30, and 60 s after light-switching at 525-nm. A small but instantaneous permeation of NMDG was detected that did not change during time illumination ($P_{NMDG}/P_{Cs} \leq 0.17$), whereas in control conditions a progressive increase of NMDG permeation was recorded following prolonged ATP application for the P2X2-3T receptor (Fig. 5*B*, Fig. S6, and Table S4). These data indicate that light-gated channels open cation-selective pores that are partially in dilated states.

Application of Optogating in Neurons. Finally, we expressed the K69A/I328C mutant in dissociated hippocampal neurons, which express P2X2 receptors (35, 36), and triggered MEA-TMA activation in the absence of putative chronic effects induced by ATP exposure. Excitation per se had no effect on background neuronal currents (Fig. 5*C*). Brief application of MEA-TMA induced robust inward currents which were rapidly and reversibly driven upon further light exposures at either 525 nm or 365 nm (Fig. 5*C*). Importantly, the currents did not change significantly when turning lights off, further demonstrating bistability of the optogating method in neurons (Fig. 5*D*). The modulation of the light-gated channels not only induced a P2X2-like current in the absence of ATP, but it also subsequently modulated the synaptic activity and action-potential firing of the hippocampal neurons (Fig. 5 *C*, *E*, and *F*). Thus, these data pave the way for dissecting in vivo the physiological and pathological roles of P2X receptors at an unprecedented level of precision.

Discussion

This study presents optogating, a unique optogenetic method in which the gating machinery of a P2X channel is reprogrammed to respond to light, enabling optical manipulation of neuronal activity. Optogating differs from current optogenetic approaches

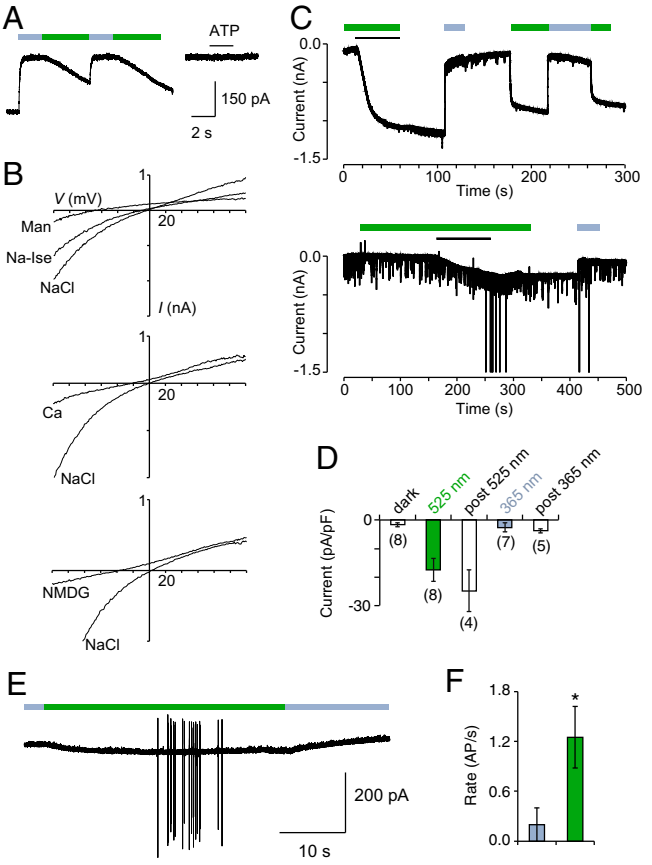

Fig. 5. An ATP-insensitive light-gated cation channel drives synaptic activity and action potential firing in neurons. (*A*) The K69A/I328C mutant tethered to MEA-TMA responds to light (*Left*), but not to ATP (*Right*, 100 μM) in HEK cells. (*B*) Current-voltage curves for the same construct recorded in different extracellular solutions in HEK cells (Man, mannitol; Na-Ise, sodium isethionate; Ca, calcium). Light-gated currents were obtained after subtracting photocurrents recorded at 525-nm light (intensity was set to 4.5 mW/mm^2) to those obtained at 365-nm light (for NMDG, current shown was recorded 60 s after light switching). (*C*) Whole-cell current from two example recordings (with moderate and robust synaptic activities) evoked by light in hippocampal neurons expressing the K69/I328C mutant following brief application of 100 μM MEA-TMA (solid lines). (*D*) Bar plot summarizing the recorded current densities (mean ± SEM for the indicated number of experiments). (*E*) Extracellular recording from hippocampal neurons expressing the K69/I328C mutant showing action-potential (AP) firing triggered by 525-nm light illumination. Cells were labeled with MEA-TMA (30 μM) under 365-nm light to maintain channels in nonconducting states. (*F*) Bar plot summarizing AP rates, defined as the number of AP per second, recorded under 365-nm light (violet bar) and 525-nm light (green bar) in experiments similar to that shown in *E* (n = 4, mean ± SEM). Rates, calculated every 5 s, were collected just before 525-nm excitation, and at the peak, within the first minute of the 525-nm excitation. Measurement of statistical significance is based on paired Student t tests; *P < 0.05.

in several ways. Optogating targets the TM gating machinery of the receptor that is known to drive opening and closing of the pore; in a sense, it substitutes ATP stimulation. Unlike optogenetic pharmacology, optogating uses photoswitchable reagents that do not target an active site. Thus, this versatile method can be extended in principle to any ion channels. More importantly, optogating relies on the possibility that receptors can be activated by light even if important biologically active or regulatory sites were genetically modified. This feature sharply contrasts with other optically controlled ligand-gated channels, such as glutamate (LiGluR) (5), $GABA_A$ (10), and nicotinic receptors (LinAChR) (6) in which endogenous neurotransmitters can still activate engineered receptors. Optogating thus provides a unique opportunity to study in native tissues the specific contribution of light-mediated signaling that is not imbalanced by the endogenous stimulus.

An important issue relies on the specificity of the optogating strategy. We showed that brief application of moderate concentrations of MEA-TMA (30–100 μM) onto neurons rapidly activated engineered channels, suggesting that this compound devoid of pharmacological specificity is quite selective in activating engineered channels. We also provide evidence that this selectivity arises from the presence of a positive charge carried by the photoswitch reagents. Although the precise stoichiometry of labeling remains unknown, our data indicate that positively charged reagents are attracted by the negatively charged vestibule located just above the pore (22, 27), enabling a covalent reaction between the maleimide and the target cysteine. The proximity-induced reaction is reminiscent of that occurring with photoswitchable affinity-labeled compounds (3, 4), ensuring the specificity of the optogating method to selectively target engineered P2X2 channels in vivo.

The qualitative similarity of the photocurrents recorded with compounds carrying either opposite or no charge suggests that toggling of tethered photoswitches is critical to the light-induced mechanism that occurs independently of ATP. We thus favor the hypothesis that the large *trans*-azobenzene repulses adjacent TM2 α-helices, resulting in pore opening, whereas the bent-shape, short *cis*-isomer enables tight association of TM2 α-helices that is necessary for closing the pore, as revealed recently by X-ray structures (22, 27) (Fig. S7). Although this proposal deserves further experimental testing, we do not exclude the possibility that the positive charge also contributes to this light-gated mechanism.

Bistability can be achieved by tethered azobenzene derivatives (3). Bistability provides a simple and nonphototoxic means to control neuronal activity by a brief pulse of light that maintains the receptor in its last tuned state for an extended period in the dark, until activity is reversed by another pulse of light of different wavelength. This landmark property is conserved in the optogating strategy, which would be suitable for in vivo applications and behavioral experiments, as previously demonstrated for other azobenzene-containing compounds (7, 37–39).

Some P2X receptors, including P2X2, are known to undergo pore dilation after prolonged application of ATP (12, 33, 34). Defined by a progressive increase (in the tens of seconds) in permeability to large organic cations, such as NMDG and propidium dyes, this process is distinct from the fast opening of the channel that occurs in the millisecond time range. Although the underlying mechanisms remain controversial (12), recent works favor a model in which pore dilation involves intrinsic conformational changes of the protein (40–42). We found that light-gated receptors open cation-selective pores that appear to be partially and stably (for at least 60 s) in dilated states, suggesting that pore-widening induced by tethered photoswitches falls between the small and large cation-selective pores.

The wide distribution of P2X2 receptors in the hippocampus (35, 43), and their established role in the regulation of excitatory neurotransmitter release onto CA1 stratum radiatum interneurons (36), stimulates the investigation of light-gated P2X receptors in neurons. We demonstrated that these engineered channels drive synaptic activity and action potential firing in hippocampal neurons rapidly and reversibly, paving the way for further studying P2X2 signaling in the brain at an unprecedented level of precision. In addition, extension of light-gated receptors to other P2X receptors, in particular to P2X4 and P2X7—two key important components involved in neuropathic pain and chronic inflammation (17, 18)—opens new possibilities for exploring the molecular links between P2X function and these debilitating disorders.

Materials and Methods

Chemical Synthesis. Synthesis of photoswitches is detailed in *SI Materials and Methods*.

Photoswitch Labeling. All photoswitch compounds except MEA-OMe were dissolved in water to make a stock solution (1–2 mM) and diluted in standard extracellular solution to 200 μM for labeling. For MEA-OMe, a solution of 80 μM was prepared in standard extracellular solution containing 1% dimethyl sulfoxide (DMSO). Increasing time incubation of MEA-TMA or MEA-OMe to 20 min prevented seal formation in the whole-cell configuration.

Molecular Modeling. Models of the rat P2X2 receptor in the active and closed state have been prepared by homology modeling using the structure of *Danio rerio* P2X4 receptor, obtained in the presence (PDB ID code 4DW1) and absence of ATP (PDB ID code 4DW0) (22) as templates, and using the software Modeler. For the I328C mutant shown in Fig. S4, the resulting model of the activated state has been superimposed with the 4DW1 structure available in the Orientations of Proteins in Membranes database (44) to get its symmetry axis superimposed with the z axis. Docking was then performed with the software AUTODOCK (45) with a constraint on the position of the charged nitrogen, which was imposed to be on the z axis successively at $z = 8$, 4, 0, and −4.

Molecular Biology and Gene Expression in Cultured Cells. Mutations were introduced into the rat P2X2 cDNA in the pcDNA3.1 expression vector as previously described (46). cDNAs encoding I328C and K69A/I328C mutants were further subcloned in the pBi-CMV3 ZsGreen bidirectional promoter vector (Clontech). All mutations were confirmed by DNA sequencing. HEK-293 cells were cultured and transiently transfected with the pcDNA3.1 vectors (0.05–0.3 μg) and a green fluorescent protein cDNA construct (0.3 μg), as described previously (46). Cultured hippocampal neurons were transfected with 1.5-μg pBi-CMV3 ZsGreen plasmids for 24–48 h, using a calcium phosphate method optimized for highly mature neuronal cultures (47).

Patch-Clamp Electrophysiology of Cultured HEK Cells. HEK-293 whole-cell patch-clamp electrophysiology was performed at room temperature (22–24 °C) 24–48 h after transfection (46). Before recordings, cells were incubated in standard extracellular solution containing a 200 μM photoswitch for 5 min in the dark at room temperature, followed by extensive wash. For mutants that showed no photoactivation effect, ATP (at the EC_{50}) was included during labeling because it is known that it increases the accessibility of residues located deep within the pore (20). Patch pipette of resistance between 3 and 5 MΩ were filled with intracellular solutions containing 140 mM CsCl, 5 mM $MgCl_2$, 5 mM EGTA, 10 mM Hepes, adjusted to pH 7.3 with NaOH. The standard extracellular solution contained 140 mM NaCl, 2.8 mM KCl, 2 mM $CaCl_2$, 2 mM $MgCl_2$, 10 mM glucose, 10 mM Hepes, adjusted to pH 7.3 with NaOH. All solutions were maintained at ~300 mOsm. Cells were voltage-clamped to −60 mV (unless otherwise indicated) using the EPC10 (HEKA) amplifier and data were digitized online using PATCHMASTER software (HEKA). Illumination of cells was achieved with Primatix's collimated LEDs directly coupled to the microscope. The system contained an UHP-Mic-LED-525 and a Mic-LED-365 with an output of 525 and 365 nm, respectively. Discrete wavelengths of light (± 5 nm) were focused on cells with a Plan Fluorite 40×, 0.6 NA objective lens (Olympus). Objective lens output intensity was measured with an integrating sphere photodiode power sensor (S142C, PM100D; Thorlabs). The measured output intensities for wavelengths for 365 and 525 nm were, respectively, 2.4 and 0.36 mW/mm^2 (unless otherwise indicated). The LEDs were controlled with TTL signals generated by the EPC10 patch-clamp amplifier. Data were fitted with a single-exponential decay equation: $I_t = I_\infty + A \exp(-t/\tau)$, where I_∞ and A are the residual current and maximal amplitude, respectively, t is the time in seconds, and τ is the time constant in seconds. ATP dose–response curves were determined as previously described (46).

Neuronal Culture. Primary cultures of hippocampal neurons were prepared as previously described (48). Briefly, hippocampi were dissected from embryonic

day 18 rat embryos, digested with 0.05% trypsin and hippocampal cells were seeded at a density of 12,000/cm^2 on poly-D-lysine (50 μg/mL; Sigma) precoated coverslips. Neurons were cultured in neurobasal medium supplemented with 2% (vol/vol) B27 (Invitrogen), 2 mM L-glutamine (Sigma), 100 U/mL Penicillin and 100 μg/mL Streptomycin antibiotics (Gibco).

Electrophysiological Recordings in Cultured Neurons. The neurons were continuously perfused with an extracellular solution containing 140 mM NaCl, 2 mM $CaCl_2$, 3 mM KCl, 10 mM Hepes, 10 mM glucose adjusted to pH 7.4 with NaOH and to 330 mOsm with Na-acetate (22–24 °C), as previously described (49). Recording pipettes were pulled from borosilicate glass and had a resistance of 3–5 MΩ when filled with a solution containing 115 mM $CsMeSO_3$, 20 mM CsCl, 10 mM Hepes, 0.6 mM EGTA, 4 mM Na_2-ATP, 0.4 mM Na-GTP, 10 mM Na-phosphocreatine, and 2.5 mM $MgCl_2$, adjusted to pH 7.2 with CsOH and to 300 mOsm with Cs-acetate (modified from ref. 50). Mature (14–16 d in vitro) hippocampal neurons expressing the transfection marker ZsGreen were visualized and recorded with the patch-clamp technique, as previously described (51). After establishing the whole-cell configuration, MEA-TMA (100 μM) was briefly applied onto the neuron from a glass pipet, located at <100-μm distance from the cell body. Steady-state light-sensitive currents at −60 mV were modulated by either exposure to UV light (350 ± 25 nm) or to green light (525 ± 25 nm) of a 100 W HBO lamp (Zeiss FluoArc). The procedure was the same for extracellular recordings of action potentials (49), except that the electrodes (2–5 MΩ) were filled with 130 mM NaCl, 2.5 mM KCl, 10 mM Hepes, 10 mM Glucose, 2 mM $CaCl_2$, 1 mM $MgCl_2$, pH 7.4 with NaOH (295 mOsm adjusted with NaCl), and that recordings were performed when tip resistance reached 100 MΩ. MEA-TMA (30 μM) was briefly applied onto the neuron, as described above.

Relative Permeability Measurements. The procedure is detailed in *SI Materials and Methods*.

ACKNOWLEDGMENTS. The authors thank Prof. Maurice Goeldner and Dr. Thierry Chataigneau for helpful discussion, and Dr. Federica Bertaso for critical reading of the manuscript and helpful discussion. This work was supported by the Centre National de la Recherche Scientifique, the Ministère de la Recherche, the International Center for Frontier Research in Chemistry, and the Agence Nationale de la Recherche (ANR 11 BSV5 001-01).

1. Deisseroth K (2011) Optogenetics. *Nat Methods* 8(1):26–29.
2. Gorostiza P, Isacoff EY (2008) Optical switches for remote and noninvasive control of cell signaling. *Science* 322(5900):395–399.
3. Fehrentz T, Schönberger M, Trauner D (2011) Optochemical genetics. *Angew Chem Int Ed Engl* 50(51):12156–12182.
4. Kramer RH, Mourot A, Adesnik H (2013) Optogenetic pharmacology for control of native neuronal signaling proteins. *Nat Neurosci* 16(7):816–823.
5. Volgraf M, et al. (2006) Allosteric control of an ionotropic glutamate receptor with an optical switch. *Nat Chem Biol* 2(1):47–52.
6. Tochitsky I, et al. (2012) Optochemical control of genetically engineered neuronal nicotinic acetylcholine receptors. *Nat Chem* 4(2):105–111.
7. Levitz J, et al. (2013) Optical control of metabotropic glutamate receptors. *Nat Neurosci* 16(4):507–516.
8. Banghart M, Borges K, Isacoff E, Trauner D, Kramer RH (2004) Light-activated ion channels for remote control of neuronal firing. *Nat Neurosci* 7(12):1381–1386.
9. Sandoz G, Levitz J, Kramer RH, Isacoff EY (2012) Optical control of endogenous proteins with a photoswitchable conditional subunit reveals a role for TREK1 in GABA (B) signaling. *Neuron* 74(6):1005–1014.
10. Yue L, et al. (2012) Robust photoregulation of GABA(A) receptors by allosteric modulation with a propofol analogue. *Nat Commun* 3:1095.
11. Szymański W, Beierle JM, Kistemaker HA, Velema WA, Feringa BL (2013) Reversible photocontrol of biological systems by the incorporation of molecular photoswitches. *Chem Rev* 113(8):6114–6178.
12. Khakh BS, North RA (2012) Neuromodulation by extracellular ATP and P2X receptors in the CNS. *Neuron* 76(1):51–69.
13. Jiang R, Taly A, Grutter T (2013) Moving through the gate in ATP-activated P2X receptors. *Trends Biochem Sci* 38(1):20–29.
14. Kaczmarek-Hájek K, Lörinczi E, Hausmann R, Nicke A (2012) Molecular and functional properties of P2X receptors—Recent progress and persisting challenges. *Purinergic Signal* 8(3):375–417.
15. Burnstock G (2008) Purinergic signalling and disorders of the central nervous system. *Nat Rev Drug Discov* 7(7):575–590.
16. White N, Burnstock G (2006) P2 receptors and cancer. *Trends Pharmacol Sci* 27(4): 211–217.
17. Di Virgilio F (2007) Liaisons dangereuses: P2X(7) and the inflammasome. *Trends Pharmacol Sci* 28(9):465–472.
18. Beggs S, Trang T, Salter MW (2012) P2X4R+ microglia drive neuropathic pain. *Nat Neurosci* 15(8):1068–1073.
19. Rassendren F, Buell G, Newbolt A, North RA, Surprenant A (1997) Identification of amino acid residues contributing to the pore of a P2X receptor. *EMBO J* 16(12): 3446–3454.
20. Li M, Chang TH, Silberberg SD, Swartz KJ (2008) Gating the pore of P2X receptor channels. *Nat Neurosci* 11(8):883–887.
21. Jiang LH, Rassendren F, Spelta V, Surprenant A, North RA (2001) Amino acid residues involved in gating identified in the first membrane-spanning domain of the rat P2X (2) receptor. *J Biol Chem* 276(18):14902–14908.
22. Hattori M, Gouaux E (2012) Molecular mechanism of ATP binding and ion channel activation in P2X receptors. *Nature* 485(7397):207–212.
23. Trujillo CA, et al. (2006) Inhibition mechanism of the recombinant rat P2X(2) receptor in glial cells by suramin and TNP-ATP. *Biochemistry* 45(1):224–233.
24. Gorostiza P, et al. (2007) Mechanisms of photoswitch conjugation and light activation of an ionotropic glutamate receptor. *Proc Natl Acad Sci USA* 104(26):10865–10870.
25. Li Z, Migita K, Samways DS, Voigt MM, Egan TM (2004) Gain and loss of channel function by alanine substitutions in the transmembrane segments of the rat ATP-gated P2X2 receptor. *J Neurosci* 24(33):7378–7386.
26. Cao L, Broomhead HE, Young MT, North RA (2009) Polar residues in the second transmembrane domain of the rat P2X2 receptor that affect spontaneous gating, unitary conductance, and rectification. *J Neurosci* 29(45):14257–14264.
27. Kawate T, Michel JC, Birdsong WT, Gouaux E (2009) Crystal structure of the ATP-gated P2X(4) ion channel in the closed state. *Nature* 460(7255):592–598.
28. Cao L, Young MT, Broomhead HE, Fountain SJ, North RA (2007) Thr339-to-serine substitution in rat P2X2 receptor second transmembrane domain causes constitutive opening and indicates a gating role for Lys308. *J Neurosci* 27(47):12916–12923.
29. Jiang R, et al. (2012) Tightening of the ATP-binding sites induces the opening of P2X receptor channels. *EMBO J* 31(9):2134–2143.
30. Browne LE, et al. (2011) P2X receptor channels show threefold symmetry in ionic charge selectivity and unitary conductance. *Nat Neurosci* 14(1):17–18.
31. Evans RJ, et al. (1996) Ionic permeability of, and divalent cation effects on, two ATP-gated cation channels (P2X receptors) expressed in mammalian cells. *J Physiol* 497(Pt 2):413–422.
32. Bo X, et al. (2003) Pharmacological and biophysical properties of the human P2X5 receptor. *Mol Pharmacol* 63(6):1407–1416.
33. Khakh BS, Bao XR, Labarca C, Lester HA (1999) Neuronal P2X transmitter-gated cation channels change their ion selectivity in seconds. *Nat Neurosci* 2(4):322–330.
34. Virginio C, MacKenzie A, Rassendren FA, North RA, Surprenant A (1999) Pore dilation of neuronal P2X receptor channels. *Nat Neurosci* 2(4):315–321.
35. Rubio ME, Soto F (2001) Distinct localization of P2X receptors at excitatory postsynaptic specializations. *J Neurosci* 21(2):641–653.
36. Khakh BS, Gittermann D, Cockayne DA, Jones A (2003) ATP modulation of excitatory synapses onto interneurons. *J Neurosci* 23(19):7426–7437.
37. Wyart C, et al. (2009) Optogenetic dissection of a behavioural module in the vertebrate spinal cord. *Nature* 461(7262):407–410.
38. Caporale N, et al. (2011) LiGluR restores visual responses in rodent models of inherited blindness. *Mol Ther* 19(7):1212–1219.
39. Szobota S, et al. (2007) Remote control of neuronal activity with a light-gated glutamate receptor. *Neuron* 54(4):535–545.
40. Chaumont S, Khakh BS (2008) Patch-clamp coordinated spectroscopy shows P2X2 receptor permeability dynamics require cytosolic domain rearrangements but not Panx-1 channels. *Proc Natl Acad Sci USA* 105(33):12063–12068.
41. Yan Z, Li S, Liang Z, Tomić M, Stojilkovic SS (2008) The P2X7 receptor channel pore dilates under physiological ion conditions. *J Gen Physiol* 132(5):563–573.
42. Browne LE, Compan V, Bragg L, North RA (2013) P2X7 receptor channels allow direct permeation of nanometer-sized dyes. *J Neurosci* 33(8):3557–3566.
43. Masin M, Kerschensteiner D, Dümke K, Rubio ME, Soto F (2006) Fe65 interacts with P2X2 subunits at excitatory synapses and modulates receptor function. *J Biol Chem* 281(7):4100–4108.
44. Lomize MA, Lomize AL, Pogozheva ID, Mosberg HI (2006) OPM: Orientations of proteins in membranes database. *Bioinformatics* 22(5):623–625.
45. Morris GM, et al. (2009) AutoDock4 and AutoDockTools4: Automated docking with selective receptor flexibility. *J Comput Chem* 30(16):2785–2791.
46. Jiang R, et al. (2010) A putative extracellular salt bridge at the subunit interface contributes to the ion channel function of the ATP-gated P2X2 receptor. *J Biol Chem* 285(21):15805–15815.
47. Jiang M, Chen G (2006) High Ca2+-phosphate transfection efficiency in low-density neuronal cultures. *Nat Protoc* 1(2):695–700.
48. Belly A, et al. (2010) CHMP2B mutants linked to frontotemporal dementia impair maturation of dendritic spines. *J Cell Sci* 123(Pt 17):2943–2954.
49. Moutin E, et al. (2012) Dynamic remodeling of scaffold interactions in dendritic spines controls synaptic excitability. *J Cell Biol* 198(2):251–263.
50. Adesnik H, Scanziani M (2010) Lateral competition for cortical space by layer-specific horizontal circuits. *Nature* 464(7292):1155–1160.
51. Baccam N, et al. (2007) Dual-level afferent control of growth hormone-releasing hormone (GHRH) neurons in GHRH-green fluorescent protein transgenic mice. *J Neurosci* 27(7):1631–1641.